Controlling single-photon Fock-state propagation through opaque scattering media

**Thomas J. Huisman · Simon R. Huisman ·
Allard P. Mosk · Pepijn W. H. Pinkse**

Abstract The control of light scattering is essential in many quantum optical experiments. Wavefront shaping is a technique used for ultimate control over wave propagation through multiple-scattering media by adaptive manipulation of incident waves. We control the propagation of single-photon Fock states through opaque scattering media by spatial phase modulation of the incident wavefront. We enhance the probability that a single photon arrives in a target output mode with a factor 30. Our proof-of-principle experiment shows that the propagation of quantum light through multiple-scattering media can be controlled, with prospective applications in quantum communication and quantum cryptography.

1 Introduction

Wavefront shaping is an adaptive technique for classical light that provides control over light propagation in

Thomas J. Huisman and Simon R. Huisman have contributed equally to this work.

T. J. Huisman · S. R. Huisman (✉) · A. P. Mosk ·
P. W. H. Pinkse
MESA+ Institute for Nanotechnology, University of Twente,
PO Box 217, 7500 AE Enschede, The Netherlands
e-mail: s.r.huisman@utwente.nl

P. W. H. Pinkse
e-mail: p.w.h.pinkse@utwente.nl
URL: www.adaptivequantumoptics.com

Present Address:
T. J. Huisman
Institute for Molecules and Materials, Radboud University
Nijmegen, Heyendaalseweg 135, 6525 AJ Nijmegen,
The Netherlands

multiple-scattering media. This technique transforms opaque scattering media to a versatile platform for creating programmable speckle patterns with correlations similar to transport through linear optical elements [1–3]. Although adaptive techniques have been introduced to quantum light [4–8], such a versatile platform as wavefront shaping is still missing for quantum light.

Light transport in a multiple-scattering medium can be considered as a linear transformation of a multi-mode system by a scattering matrix, which results generally in a speckle pattern [9–11]. Each far-field speckle spot represents a single output mode of the system. In wavefront shaping, the incident wavefront is typically phase modulated with a spatial light modulator that controls many of thousands of individual elements. In this way, the degree of mode-mixing of all scattered waves that contribute to the target speckle spots is controlled. Recent wavefront-shaping experiments have transformed opaque media in equivalents of waveguides and lenses [2], optical pulse compressors [12, 13], and programmable waveplates [14] that are inherently flexible in performance.

Multiple scattering is also an exciting platform for quantum optical experiments [15–20]. Non-classical correlations are observed, even for opaque scattering media [15, 20–22]. We have started a series of experiments to control quantum interference in multiple-scattering materials by wavefront shaping. Controlling single-photon propagation opens unique opportunities for quantum patterning [23], secure key generation [24], or addressing quantum transport through disordered media [22].

In this article, we report the first experimental demonstration of optimizing the propagation of quantum light through a random scattering medium by wavefront shaping. We control light propagation of single-photon Fock states $|1\rangle$ through a layer of white paint. We observe that

the probability that a single-photon Fock state arrives in a target speckle spot is enhanced by a factor of 30.

2 Experimental setup for creating single-photon Fock states

A schematic of our quantum-light source is shown in Fig. 1. The quantum-light source is based on earlier work reported by Refs. [25, 26], which gives the opportunity to engineer quantum states up to the two-photon level. A mode-locked Ti:Sapphire laser (Spectra-Physics, Tsunami) emits transform-limited pulses at a repetition rate of 80 MHz with a pulse duration of (0.30 ± 0.02) ps (FWHM of the intensity envelope) and a center wavelength of 790.0 nm. Typically, 600 mW is incident on a 5-mm-long BBO nonlinear crystal cut for type I frequency doubling. After spectral and spatial filtering, about 70 mW of the frequency-doubled light pulses is focused in a 2-mm-long periodically poled KTP (PPKTP) crystal cut for type II spontaneous parametric down-conversion (SPDC) in a single-pass configuration. The polarization-entangled output state can be approximated by:

$$|\Psi\rangle \approx \sqrt{(1 - \gamma^2)}|0,0\rangle + \gamma|1,1\rangle, \tag{1}$$

where states beyond the single-photon level are omitted. The kets are labeled by the photon numbers in the separate polarization modes, and the constant $\gamma \ll 1$ is proportional to the pump field amplitude and the effective nonlinear susceptibility of the PPKTP crystal. The produced light generated by SPDC is filtered with a bandpass filter with a bandwidth of approximately 1.5 nm. The modes are separated with a polarizing beam splitter cube (PBS) from which the reflection is used as trigger mode and the transmission as signal mode. Both modes are coupled to single-mode fibers, and the fiber of the trigger mode is connected to a single-photon counting module (SPCM$_1$). Click rates were detected up to $8 \times 10^5\, \text{s}^{-1}$. Coincidence measurements with two detectors and a beam splitter in one of the output arms confirmed that a detection event corresponds to a detection of state $|1\rangle$ with a probability of (98 ± 1) %. A Hong-Ou-Mandel (HOM) dip was observed with a visibility of 38 %, where the visibility is limited because of the broad single-photon spectrum produced with type II SPDC. Strictly speaking, a visibility over 50 % is required to prove the existence of single-photon states. The mere presence of the dip which has a visibility close to what we expect [27], the ease of obtaining it, and since this type of quantum-light source is used as a standard method to produce single-photon Fock states provides sufficient indication that we are dealing with single photons. The dip visibility was independent of the incident pump power,
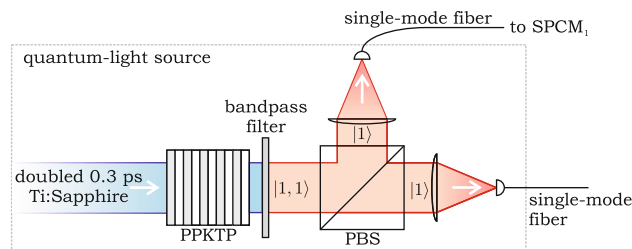
Fig. 1 Used quantum-light source. Entangled photon pairs generated in the PPKTP crystal are separated by a polarizing beam splitter cube (PBS). One photon is fiber coupled to a single-photon counting module (SPCM$_1$). The conjugate photon is fiber coupled to different types of spatial modulation setups, as shown in consecutive figures

indicating that states beyond the single-photon level can indeed be ignored in our experiment. Further characterization of the source can be found in Ref. [28]. The fiber-coupled signal mode is directed to different types of spatial modulation setups, as will be discussed in consecutive sections.

3 Spatial light modulation of single-photon Fock states

We first demonstrate in Fig. 2 the capability of programming the wavefront of single photons using spatial phase modulation. For this purpose, we use the diffraction setup presented in Fig. 2(a), in which single-photon states can enter through the single-mode fiber on the left in the figure. This mode is incident on a spatial light modulator (SLM, Hamamatsu LCOS-SLM), enabling to program the spatial phase pattern of this mode. Using a flip mirror and a 250-mm lens, the SLM pattern is either Fourier-transformed imaged onto a CCD camera or onto a multi-mode fiber connected to SPCM$_2$. Figure 2b shows the intended diffraction pattern, consisting of three bright bars. Figure 2c shows the Fourier-transformed SLM pattern on a CCD camera using a lens for incident laser pulses that act as an alignment field for the single photons. The three bars are clearly visible, where the software from the company Holoeye used to determine the diffraction patterns written to the SLM, gives rise to a spatially fluctuating intensity distribution of the bars. After we stored the corresponding phase pattern on the SLM for each of the three bars separately, the incident classical laser pulses are replaced with single photons, and the CCD camera is replaced with a multi-mode fiber with a 62.5 μm core diameter connected with SPCM$_2$. The fiber is scanned over the line indicated in Fig. 2(c) to detect the coincidence count rate as a function of position. The results are shown in Fig. 2(d). Each measurement is performed with a different SLM pattern corresponding to one of the three bars only, in order to demonstrate the ability to program the pattern, and to
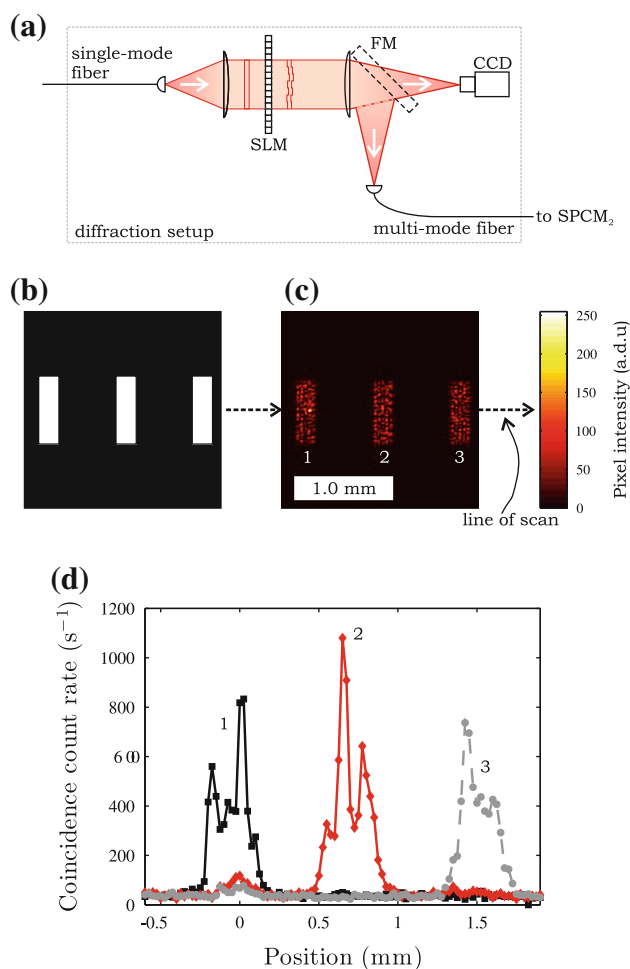
Fig. 2 Programmable single-photon diffraction patterns. **a** A diffraction setup was used in order to demonstrate spatial control over single-photon states. **b** Target diffraction pattern consisting of 3 bars. **c** Measured diffraction pattern imaged on a CCD camera for laser pulses. **d** Measured coincidence count rate for single-photon diffraction when a multi-mode fiber is scanned over the *line* indicated in **c**. *Each bar is imaged separately (black, red, gray dashed)*

Fig. 3 Wavefront-shaped single-photon speckle. **a** A wavefront-shaping setup was used in order to control the propagation of single-photon states through multiple-scattering media. **b** Speckle pattern imaged on a CCD camera for classical laser pulses with a random phase pattern. The circle indicates the target for optimization. **c** Speckle pattern with a single enhanced mode for an optimized phase pattern. **d** Measured coincidence count rate at the position of the bright speckle spot in **c** for an optimized (*red*), constant (*gray*), and random phase patterns (*white*). The *blue dashed line* represents the average coincidence rate measured for random phase patterns. The errors are taken as 2 times the standard deviations

improve the observed coincidence count rate per bar by roughly a factor three. The coincidence count rate is clearly highest in the intended regions and shows similar spatial intensity fluctuations as observed for laser light.

4 Wavefront shaping of single-photon Fock states through white paint

Figure 3 shows the main result of this article: spatial control of single-photon propagation through a multiple-scattering medium by wavefront shaping. For this result, we used the setup as presented in Fig. 3a, in which single-photon states enter through the single-mode fiber on the left. This mode is incident on a SLM and focused on a layer of white paint with an objective (NA = 0.95). The
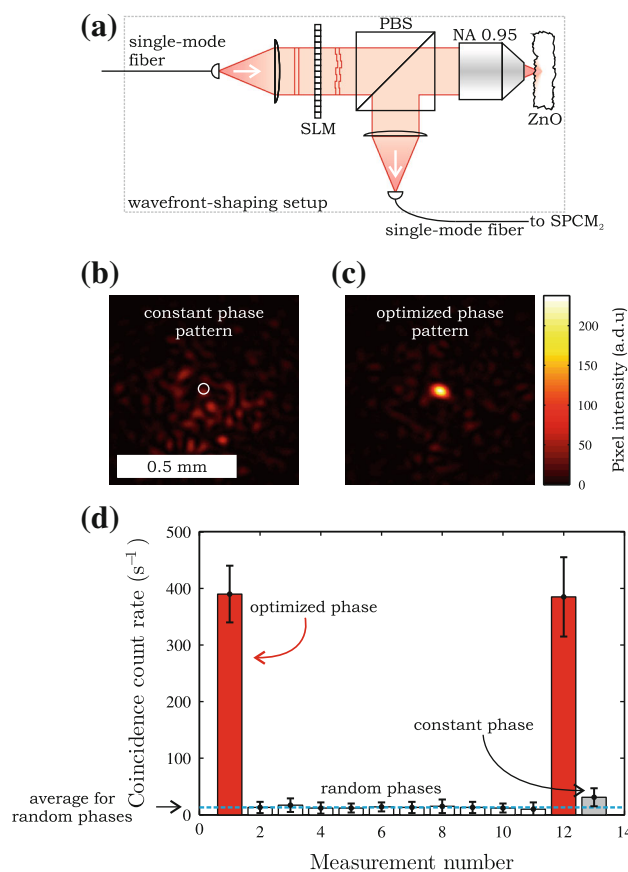
modulated wavefront propagates freely between the SLM and the objective over a distance of approximately 0.8 meter. The layer of white paint consists of ZnO powder with a scattering mean free path of (0.7 ± 0.2) μm. The reflected speckle pattern is collected with the same objective and polarization filtered with a polarizing beam splitter cube to select multiple-scattered light, making the detection mainly sensitive for light that went through the medium. One of the speckle spots is coupled to a single-mode fiber that is connected to SPCM$_2$. The wavefront-shaping setup is based on the configuration described in Ref. [2], with the main difference that we use a reflection configuration. The reflection configuration is expected to give a higher collection efficiency of the scattered modes [24]. The results presented in this article have been reproduced

by us in a transmission configuration (not shown), which indeed resulted in a collection efficiency reduced by more than an order of magnitude compared to the reflection configuration.

We first use laser pulses to create an optimized classical speckle pattern with a single enhanced speckle spot. The beam is phase modulated by approximately 500 segments consisting of 20×20 pixels. Each segment is sequentially addressed with a random phase. Only if the intensity increased, this new phase was accepted. One such measurements took about 0.5 s. This algorithm was repeated approximately 5 times for all segments, with an approximate total duration of half an hour to obtain a single enhanced speckle spot. Figure 3(b) shows the speckle pattern for a constant phase pattern, and Fig. 3c shows the pattern after optimization. These camera images were taken by putting a CCD camera in the focal length of a 200-mm lens, while the speckles propagated over more than 20 cm before reaching this 200-mm lens or the single-mode fiber. A clear enhanced speckle spot is visible in the center of the image, which decreases less than 10 % in intensity in 24 h, indicating the high stability of our setup.

Figure 3(d) shows the result with incident single photons for the same realization. The camera was removed, and the target mode is coupled to a single-mode fiber that is connected with $SPCM_2$. Figure 3(d) presents the coincidence count rate for different phase patterns; optimized (red), random (white), and constant (gray). Twenty subsequent measurements of 1 second integration time were performed for each bar. From the optimized phase pattern, we obtain a coincidence count rate which is 30 ± 10 times higher than the average coincidence count rate for random phase patterns. This value is in good agreement with the measured intensity enhancement for incident laser pulses extracted from the CCD image in Fig. 3(c). This is in line with our expectation, since both single-photon states and classical light have been redistributed in the wavefront-shaping process similar to the diffraction patterns we showed in the previous section, which appeared to be identical for both single-photon states and classical light. Since the SLM surface is not imaged directly on the back aperture of the objective, the spot size illuminating the sample may likely be smaller for a constant phase pattern than for structured phase patterns, resulting into a lower intensity for structured phase patterns. However, the main difference in coincidence rate between constant and random phase patterns is the result of initially choosing a bright speckle spot to enhance. The optimized phase pattern provides a reproducible coincidence rate as indicated by the second red bar in Fig. 3(d), showing again the high stability of our setup. We have, hence, increased the probability for a single photon to appear in a desired mode 30-fold, demonstrating the capability of coupling quantum light to a desired mode after propagation through a random scattering material by wavefront shaping. This corresponds to an overall mode transmission of the order of 1 %, based on the total number of speckle spots of order 10^3 and the 30-fold enhancement. The total number of speckle spots was estimated from the amount of observed speckle spots collected by the objective. By taking into account the numerical aperture of the objective and that only a single linear polarization state is detected, we extrapolated the total number of speckle spots that are emitted in 4π sr. solid angle. Based on energy conservation and the high purity of our photon source, the detected coincidences occur when the incident wavefront and the optimized target speckle spot contained a single photon.

5 Conclusions

In summary, we have controlled single-photon propagation through opaque scattering media with spatial phase modulation of the incident light. This opens new opportunities to address elements of the scattering matrix to obtain desired quantum interference. We anticipate that our methods and findings are not limited to single-photon Fock states, but can be applied to non-classical light in general, providing new ways to perform quantum optical experiments.

References

1. I. Freund, Phys. A. **168**, 49 (1990)
2. I.M. Vellekoop, A.P. Mosk, Opt. Lett. **32**, 2309 (2007)
3. A.P. Mosk, A. Lagendijk, G. Lerosey, M. Fink, Nat. Phot. **6**, 283 (2012)
4. B. Dayan, A. Pe'er, A.A. Friesem, Y. Silberberg, Phys. Rev. Lett. **93**, 023005 (2004)
5. S. Viciani, A. Zavatta, M. Bellini, Phys. Rev. A **69**, 053808 (2004)
6. J.F. Chen, S. Zhang, H. Yan, M.M.T. Loy, G.K.L. Wong, S. Du, Phys. Rev. Lett. **104**, 183604 (2010)
7. D. Bonneau et al., Phys. Rev. Lett. **108**, 053601 (2012)
8. C. Polycarpou, K.N. Cassemiro, G. Venturi, A. Zavatta, M. Bellini, Phys. Rev. Lett. **109**, 053602 (2012)
9. P. Sheng, Introduction to wave scattering, localization, and mesoscopic phenomena. (Academic Press, Waltham, 1995)
10. C.W.J. Beenakker, Rev. Mod. Phys. **69**, 731 (1997)
11. E. Akkermans, G. Montambaux, Mesoscopic physics of electrons and photons. (Cambrigde University Press, Cambridge, 2007)
12. J. Aulbach, B. Gjonaj, P.M. Johnson, A.P. Mosk, A. Lagendijk, Phys. Rev. Lett. **106**, 103901 (2011)
13. O. Katz, E. Small, Y. Bromberg, Y. Silberberg, Nat. Phot. **5**, 372 (2011)

14. Y. Guan, O. Katz, E. Small, J. Zhou, Y. Silberberg, Opt. Lett. **37**, 4663 (2012)
15. S. Smolka, A. Huck, U.L. Andersen, A. Lagendijk, P. Lodahl, Phys. Rev. Lett. **102**, 193901 (2009)
16. Y. Bromberg, Y. Lahini, R. Morandotti, Y. Silberberg, Phys. Rev. Lett. **102**, 253904 (2009)
17. A. Peruzzo et al., Science **329**, 1500 (2010)
18. L. Sapienza et al., Science **327**, 1353 (2010)
19. Y. Lahini, Y. Bromberg, D.N. Christodoulides, Y. Silberberg, Phys. Rev. Lett. **105**, 163905 (2010)
20. W.H. Peeters, J.J.D. Moerman, van M.P. Exter, Phys. Rev. Lett **104**, 173601 (2010)
21. P. Lodahl, A.P. Mosk, A. Lagendijk, Phys. Rev. Lett. **95**, 173901 (2005)
22. J.R. Ott, N.A. Mortensen, P. Lodahl, Phys. Rev. Lett. **105**, 090501 (2010)
23. A.N. Boto et al., Phys. Rev. Lett. **85**, 2733 (2000)
24. S.A. Goorden, M. Horstmann, A.P. Mosk, B. Škorić, Pinkse P.W.H., ArXiv **1303.0142**, (2013)
25. S.R. Huisman et al., Opt. Lett. **34**, 2739 (2009)
26. E. Bimbard, N. Jain, A. MacRae, A.I. Lvovsky, Nat. Phot. **4**, 243 (2010)
27. W.P. Grice, I.A. Walmsley, Phys. Rev. A **56**, 1627 (1997)
28. T.J. Huisman, S.R. Huisman, A.P. Mosk, P.W.H. Pinkse, ArXiv **1302.2816** (2013)